# Electronic Supplementary Material

# Room-temperature hydrogenation of halogenated nitrobenzenes over metal-organic-framework-derived ultra-dispersed Ni stabilized by N-doped carbon nanoneedles

Yuemin Lin[1], Yuanyuan Zhang[1], Renfeng Nie (✉)[2], Kai Zhou[1], Yao Ma[1], Mingjie Liu[1], Dan Lu[1], Zongbi Bao[1,3], Qiwei Yang[1,3], Yiwen Yang[1,3], Qilong Ren[1,3], Zhiguo Zhang (✉)[1,3]

1 Key Laboratory of Biomass Chemical Engineering of Ministry of Education, College of Chemical and Biological Engineering, Zhejiang University, Hangzhou 310027, China

2 School of Chemical Engineering, Henan Center for Outstanding Overseas Scientists, Zhengzhou University, Zhengzhou 450001, China

3 Institute of Zhejiang University-Quzhou, Quzhou 324000, China

E-mails: zhiguo.zhang@zju.edu.cn (Zhang Z); rnie@zzu.edu.cn (Nie R)

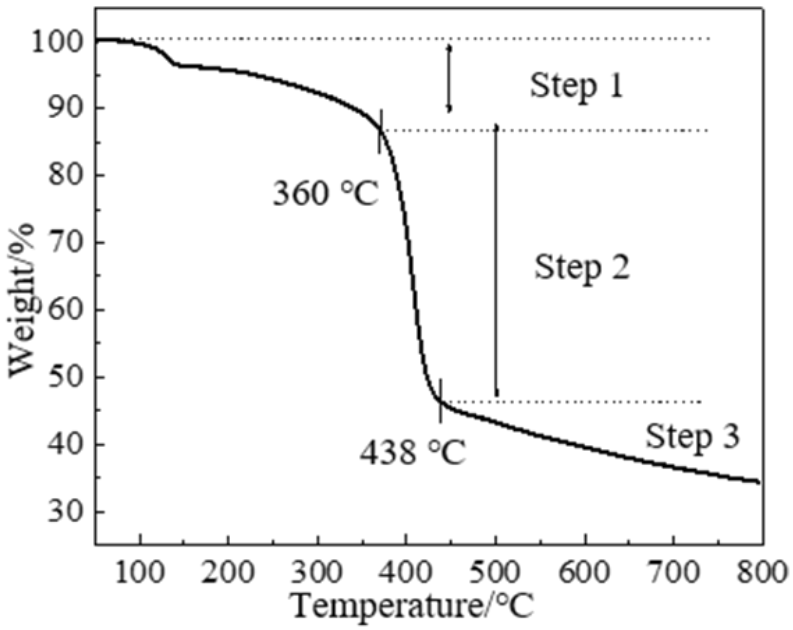


**Fig. S1** Thermogravimetric curve for Ni-MOF$_{stirring}$ in $N_2$ atmosphere with a ramping rate of 10 °C min$^{-1}$.

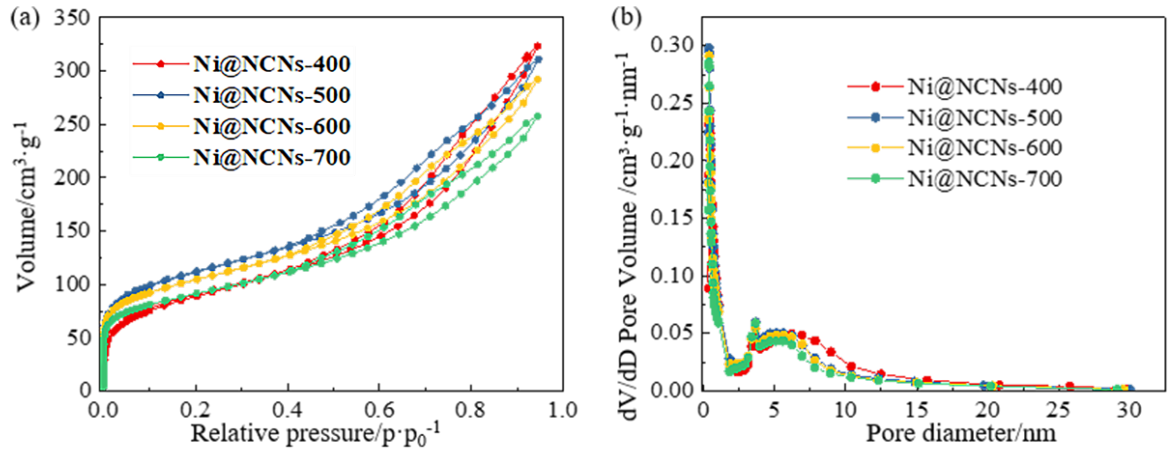


**Fig. S2** (a) $N_2$ adsorption-desorption isotherms of Ni@NCNs-T at 77 K. (b) Pore size distributions of Ni@NCNs-T.

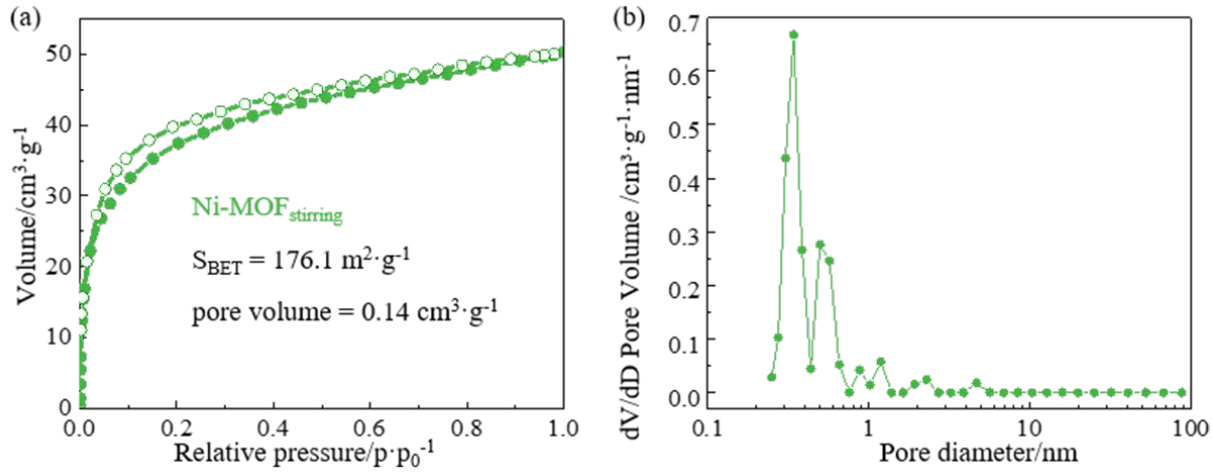


**Fig. S3** (a) $CO_2$ adsorption-desorption isotherms of Ni-$MOF_{stirring}$ at 195 K. (b) Pore size distribution of Ni-$MOF_{stirring}$.

**Table S1** Specific surface area and pore structure of Ni@NCNs-T [a)]

| Catalysts | $S_{BET}$ /m²·g⁻¹ | pore volume /cm³·g⁻¹ | micropores size/nm | mesopores size/nm |
|---|---|---|---|---|
| Ni@NCNs-400 | 316.3 | 0.50 | 0.494 | 6.75 |
| Ni@NCNs-500 | 384.6 | 0.48 | 0.413 | 6.00 |
| Ni@NCNs-600 | 359.8 | 0.45 | 0.397 | 5.93 |
| Ni@NCNs-700 | 314.2 | 0.40 | 0.391 | 5.91 |

a) Detected by $N_2$ adsorption-desorption.

**Table S2** Elemental percentage of C, N, H and Ni in Ni@NCNs-T

| Sample | C/wt. % [a)] | N/wt. % [a)] | H/wt. % [a)] | Ni/wt. % [b)] |
|---|---|---|---|---|
| Ni@NCNs-400 | 28.93 | 6.39 | 2.22 | 47 |
| Ni@NCNs-500 | 26.64 | 6.19 | 1.70 | 49 |
| Ni@NCNs-600 | 20.20 | 3.30 | 0.92 | 51 |
| Ni@NCNs-700 | 10.36 | 1.37 | 0.26 | 59 |

a) Detected by element analysis.; b) Detected by inductively coupled plasma optical emission spectrometry (ICP-OES) analysis.

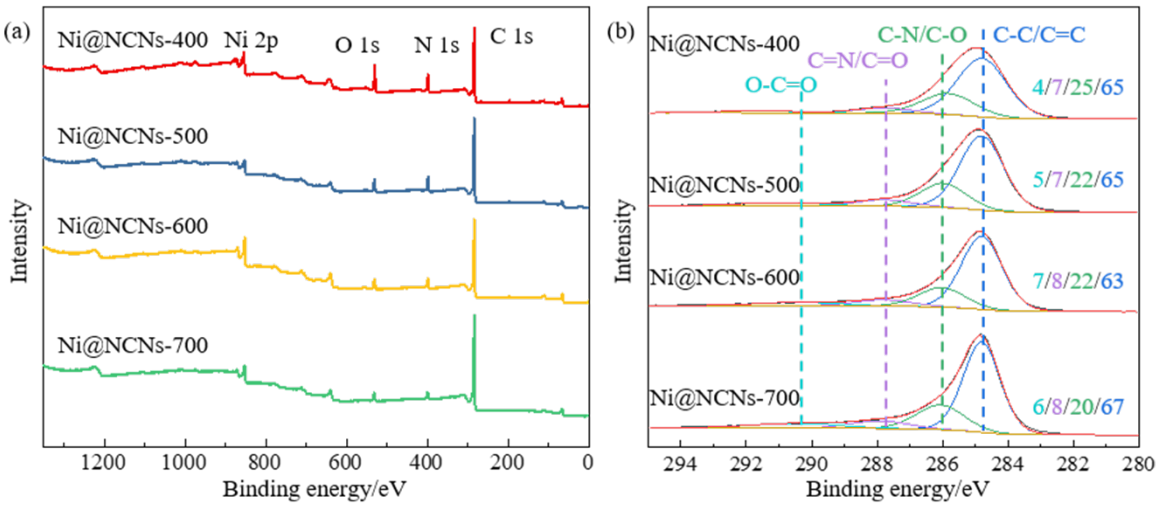


**Fig. S4** X-ray photoelectron spectroscopy (XPS) survey (a) and C 1*s* spectra (b) of Ni@NCNs-T.

**Table S3** The content of surface elements in Ni@NCNs-T [a)]

| Sample | C% | N/% | O/% | Ni/ % |
|---|---|---|---|---|
| Ni@NCNs-400 | 71.2 | 11.8 | 12.0 | 4.95 |
| Ni@NCNs-500 | 78.7 | 11.2 | 6.9 | 3.2 |
| Ni@NCNs-600 | 79.4 | 9.1 | 6.3 | 5.3 |
| Ni@NCNs-700 | 85.5 | 6.7 | 4.7 | 3.2 |

a) Atomic concentrations were detected in XPS analysis

**Table S4** Comparison of the catalytic performance of reported Ni-based catalysts for *p*-chloronitrobenzene hydrogenation to *p*-chloroaniline.

| Catalysts | T/°C | $H_2$ Pressure /MPa | Reaction Time | Conv./% | Catalytic productivity /$h^{-1}$ [a)] | Sele./% | Ref. |
|---|---|---|---|---|---|---|---|
| Ni@NCNsNs-600 | 90 | 1.5 | 20 min | 100 | 77.9 | 99.3 | *This work* |
| Ni@NCNsNs-600 | r.t. | 1 | 20 h | 100 | 1.3 | 100 | *This work* |
| Ni–P/CNTs-MA | 110 | 3 | 1.7 h | 98.9 | 29.1 | 98.6 | [1] |

| | | | | | | | |
|---|---|---|---|---|---|---|---|
| Ni-N-C-700 | 120 | 3 | 8 h | 100 | 8.4 | 99.0 | [2] |
| Ni@C-N/$SiO_2$ | 110 | 1.1 | 75 min | 100 | 9.0 | 100 | [3] |
| Ni/$CeO_2$-CAS | 210 | 2 | 7 h | 100 | 3.7 | 99.5 | [4] |
| Ni@C-650 | 140 | 0.5 | 40 min | 100 | 12.6 | 94.3 | [5] |
| Ni-B-in/CNT | 140 | 2 | 1 h | 76.2 | 19.5 | 93.6 | [6] |
| Ni@$PS_{60}$SiCN | 110 | 5 | 20 h | 100 | 5.0 | > 99 | [7] |
| Ni/LaMCM-41-$NH_2$ | 70 | 2 | 3 h | 100 | 8.3 | 99.8 | [8] |
| Ni/$TiO_2$@OAC | 70 | 2 | 4 h | 100 | 9.4 | 98.7 | [9] |
| Ni@CN-500 | 60 | 2 | 3 h | 94 | 4.3 | 92.1 | [10] |

a) The catalytic productivity is defined as the mole of converted *p*-chloronitrobenzene per mole of Ni per hour.

## NMR Data of the Products

**(1) *p*-Chloroaniline**

$^1$H NMR (400 MHz, $CDCl_3$) δ 7.12-7.08 (m, 2H), 6.62-6.59 (m, 2 H), 3.65 (s, 2H).

$^{13}$C NMR (100 MHz, $CDCl_3$) δ 144.93, 129.12, 123.16, 116.23.

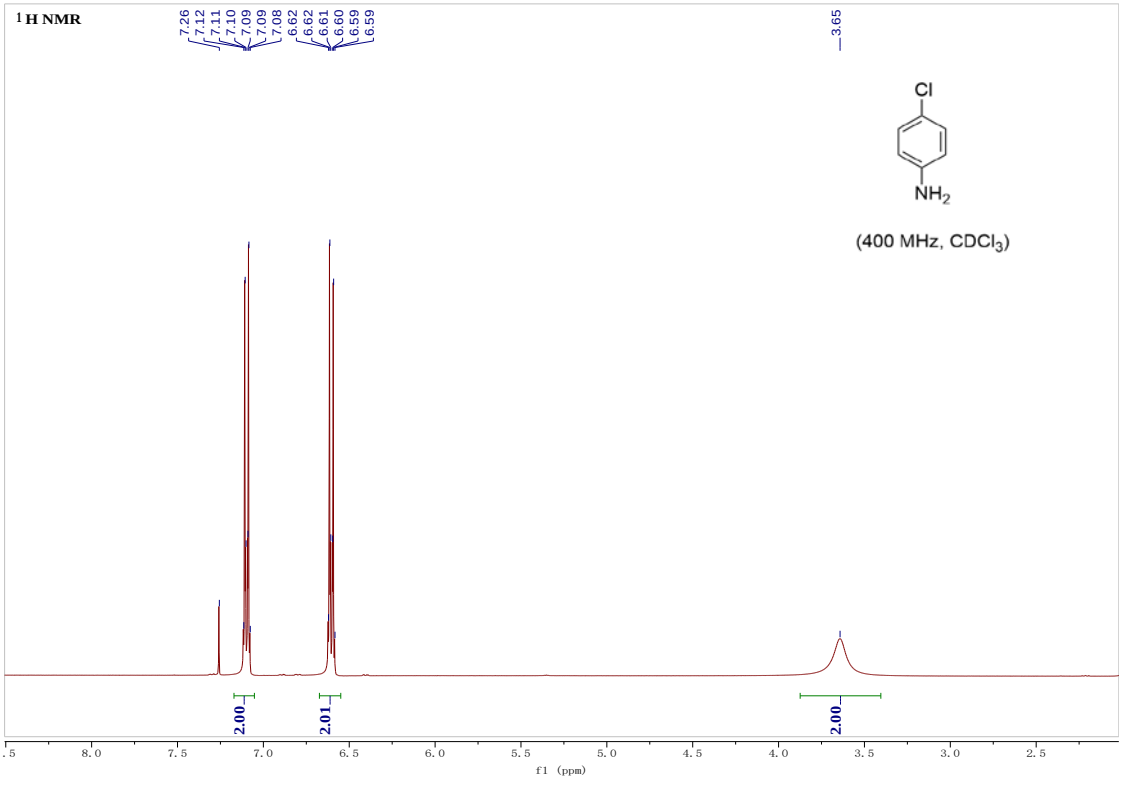

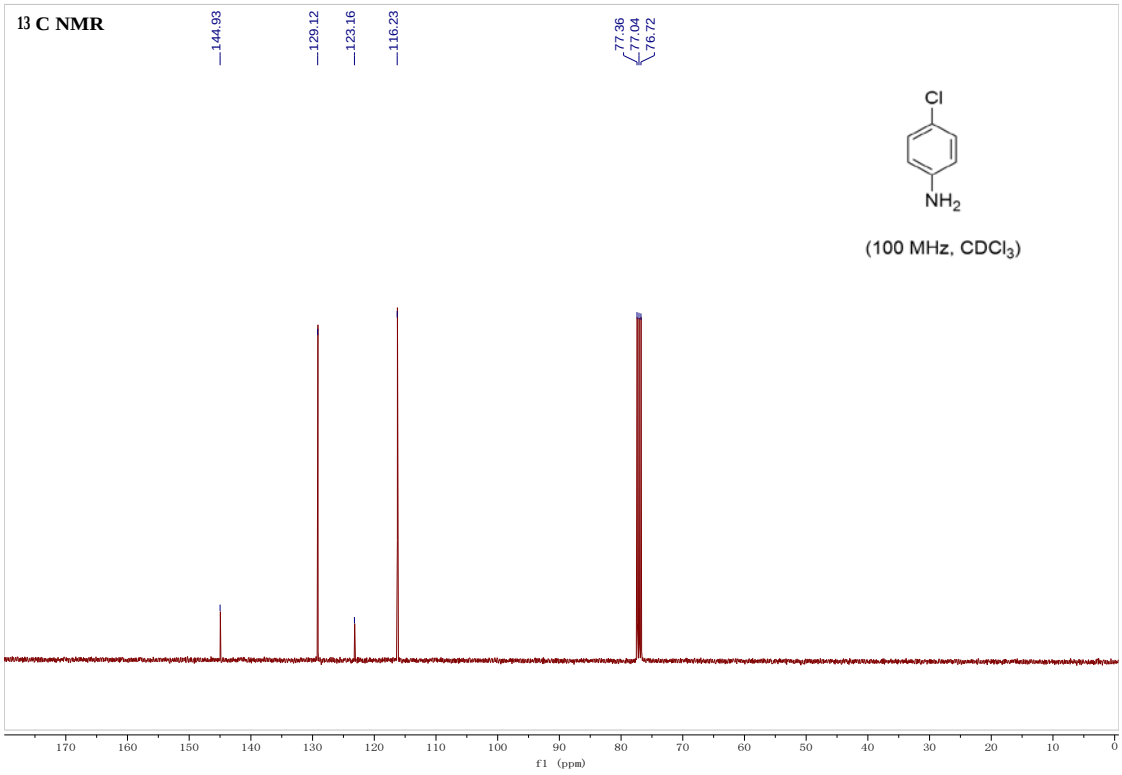


**(2) *m*-Chloroaniline**

$^{1}$H NMR (400 MHz, $CDCl_3$) δ 7.06 (t, *J* = 8.0 Hz, 1H), 6.73-6.66 (m, 2H), 6.54 (dd, *J* = 8.0, 1.6 Hz, 1H), 3.70 (s, 2H).

$^{13}$C NMR (100 MHz, $CDCl_3$) δ 147.60, 134.83, 130.31, 118.49, 114.95, 113.22.

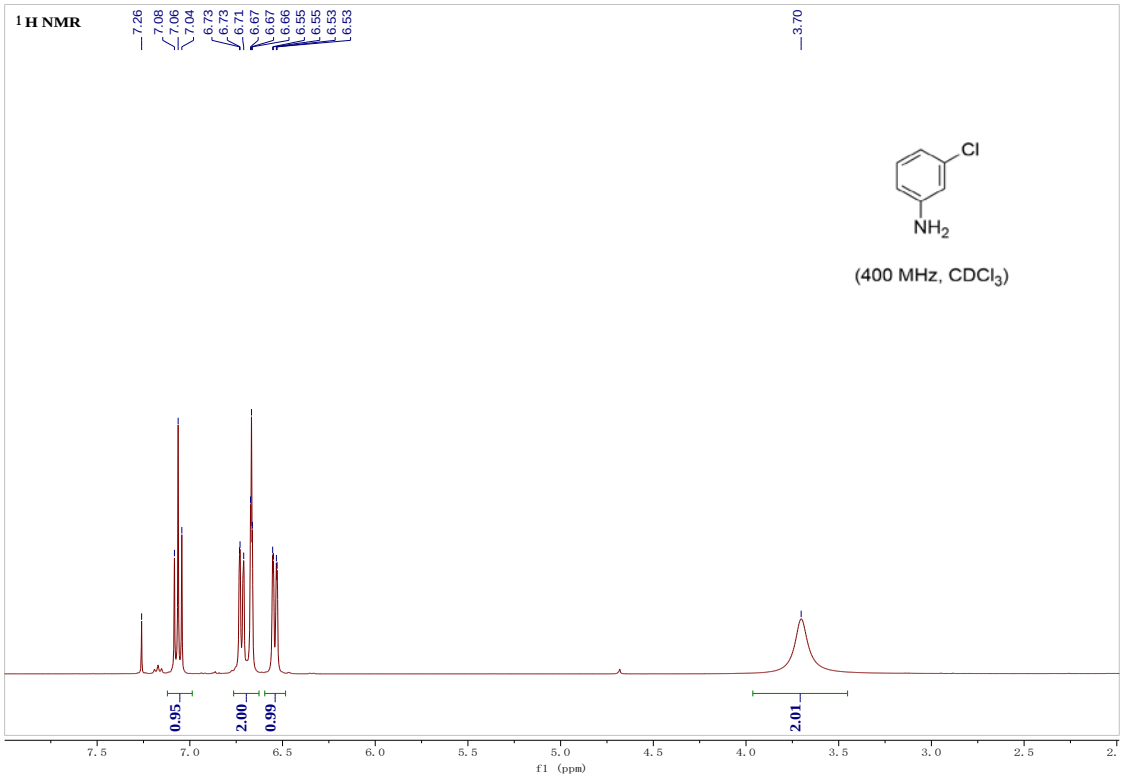

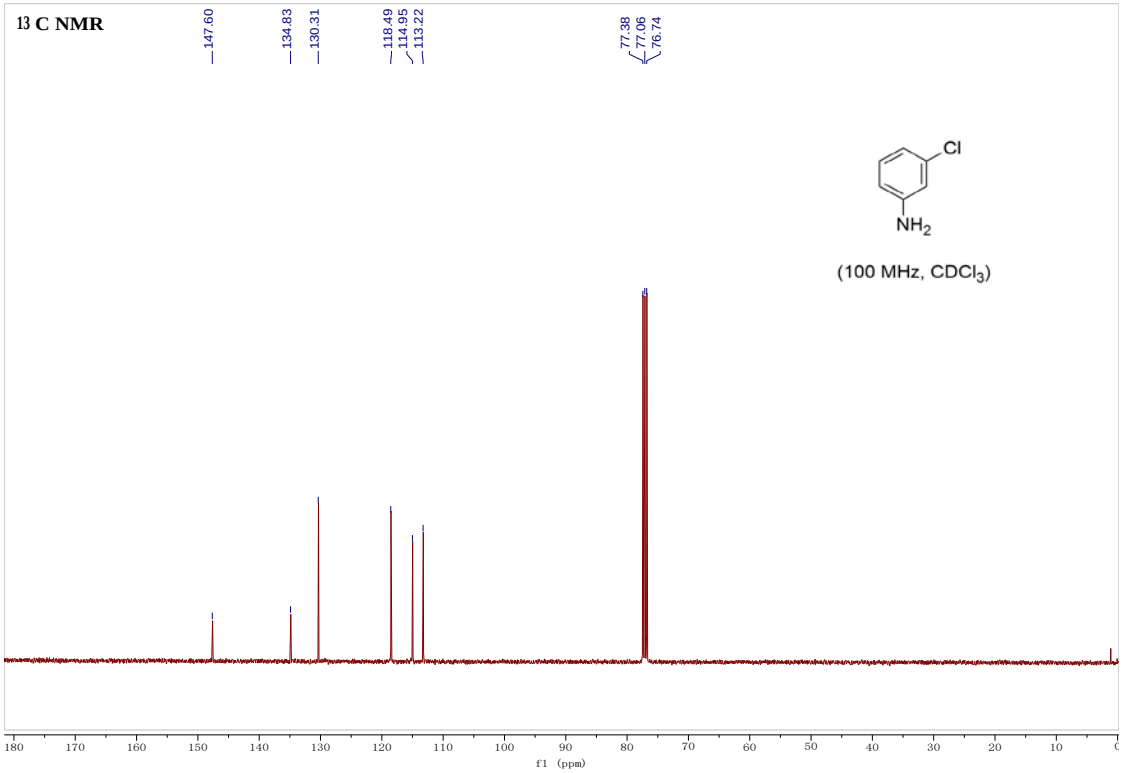


**(3) *o*-Chloroaniline**

$^{1}$H NMR (400 MHz, $CDCl_3$) δ 7.24 (dd, *J* = 8.0, 1.4 Hz, 1 H), 7.08-7.04 (m, 1H), 6.76 (dd, *J* = 8.0, 1.4 Hz, 1H), 6.69 (td, *J* = 7.8, 1.4 Hz, 1H), 4.02 (s, 2H).

$^{13}$C NMR (100 MHz, $CDCl_3$) δ 142.88, 129.41, 127.62, 119.30, 119.03, 115.86.

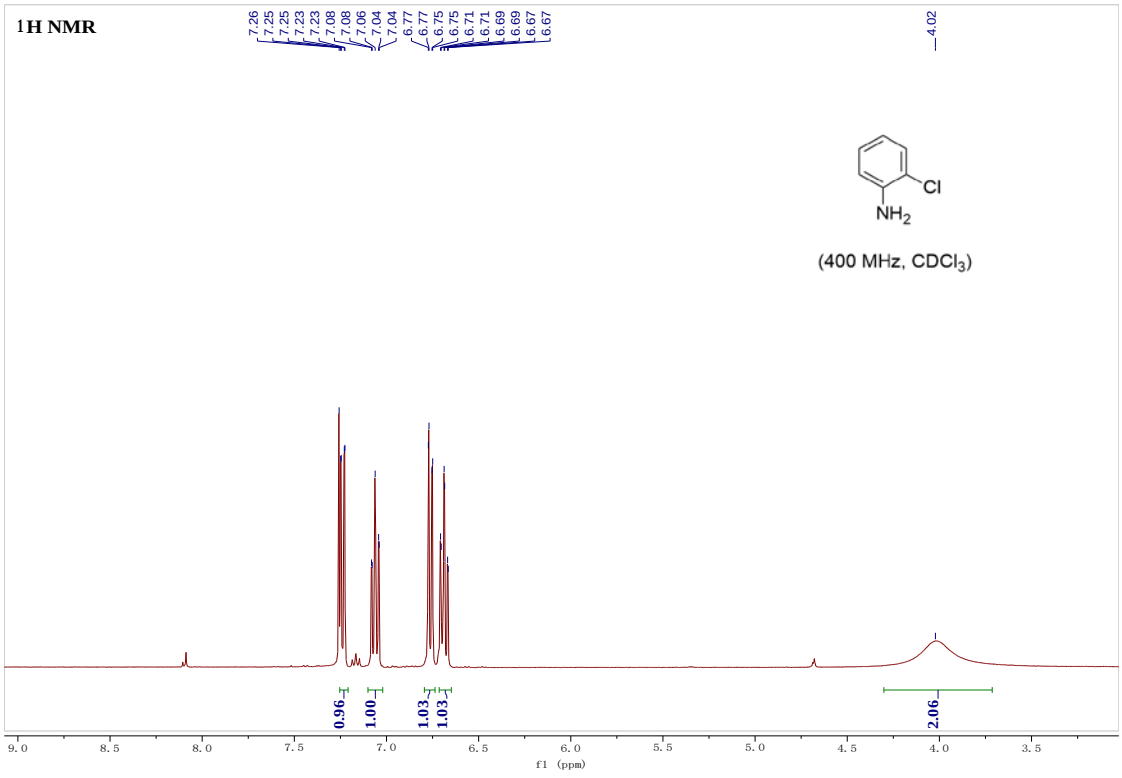

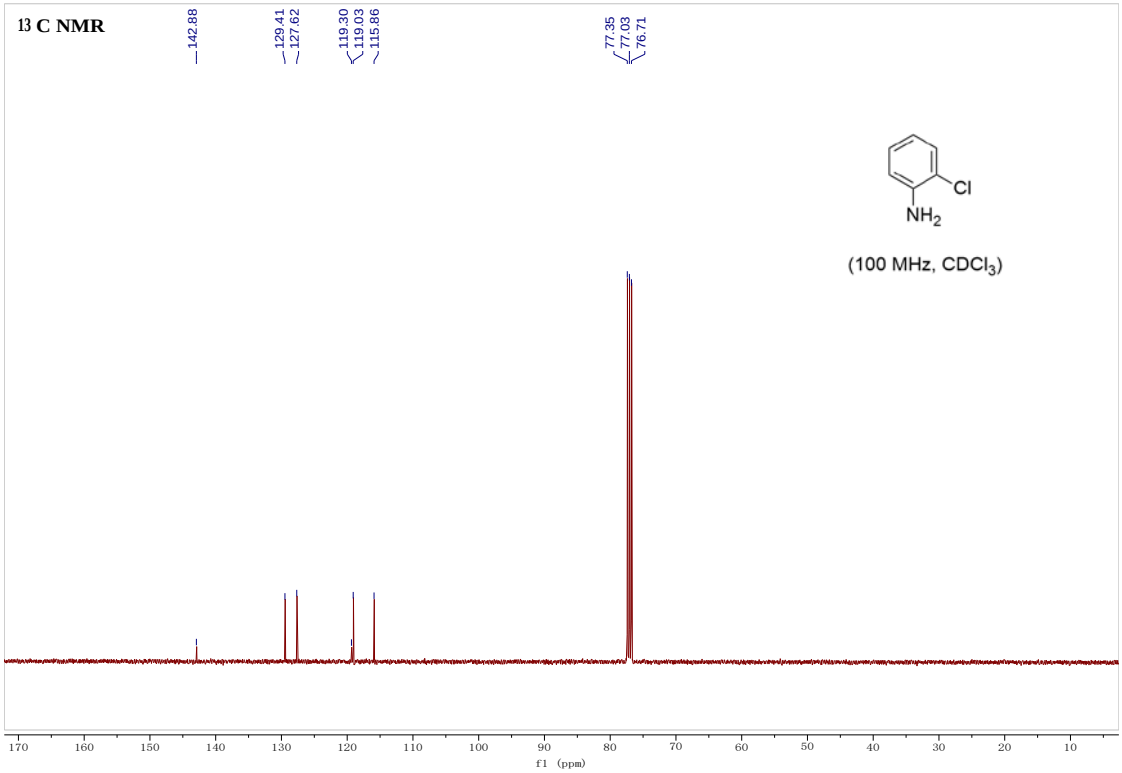


**(4) *o*-Bromoaniline**

$^{1}$H NMR (400 MHz, $CDCl_3$) δ 7.41 (d, *J* = 8.0 Hz, 1H), 7.13-7.09 (m, 1H), 6.77 (dd, *J* = 8.0, 1.4 Hz, 1H), 6.65-6.60 (m, 1H), 4.08 (s, 2H).

$^{13}$C NMR (100 MHz, $CDCl_3$) δ 144.07, 132.59, 128.36, 119.43, 115.77, 109.34.

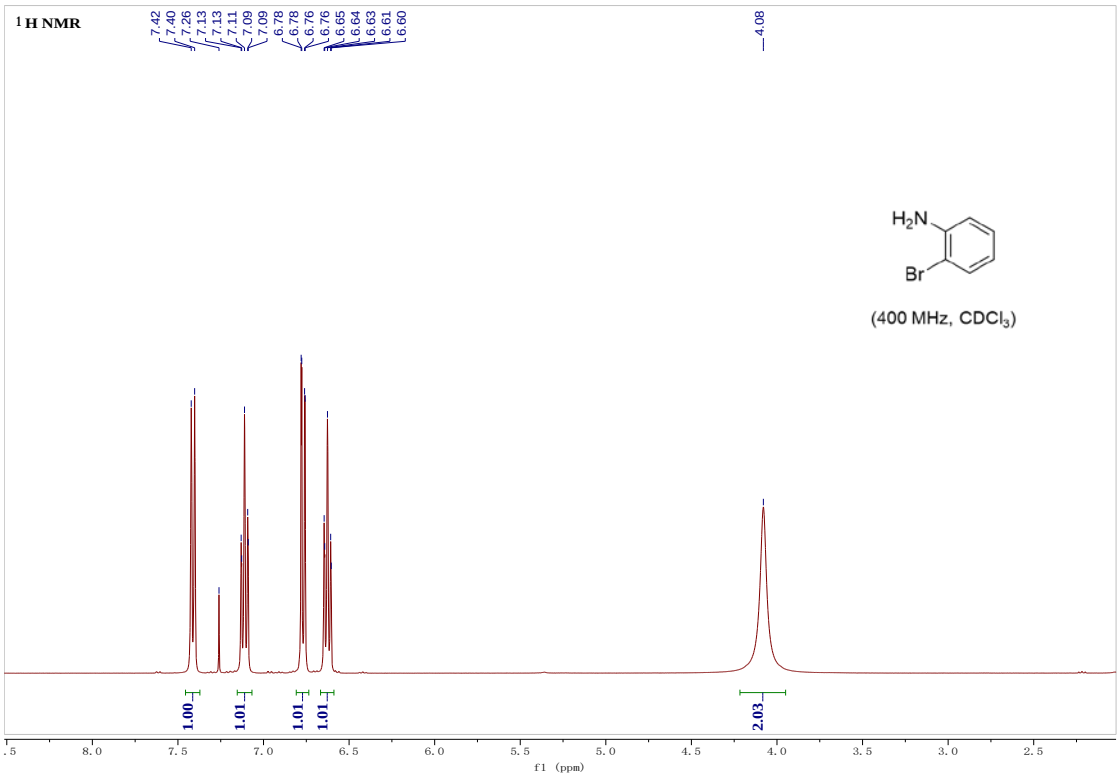

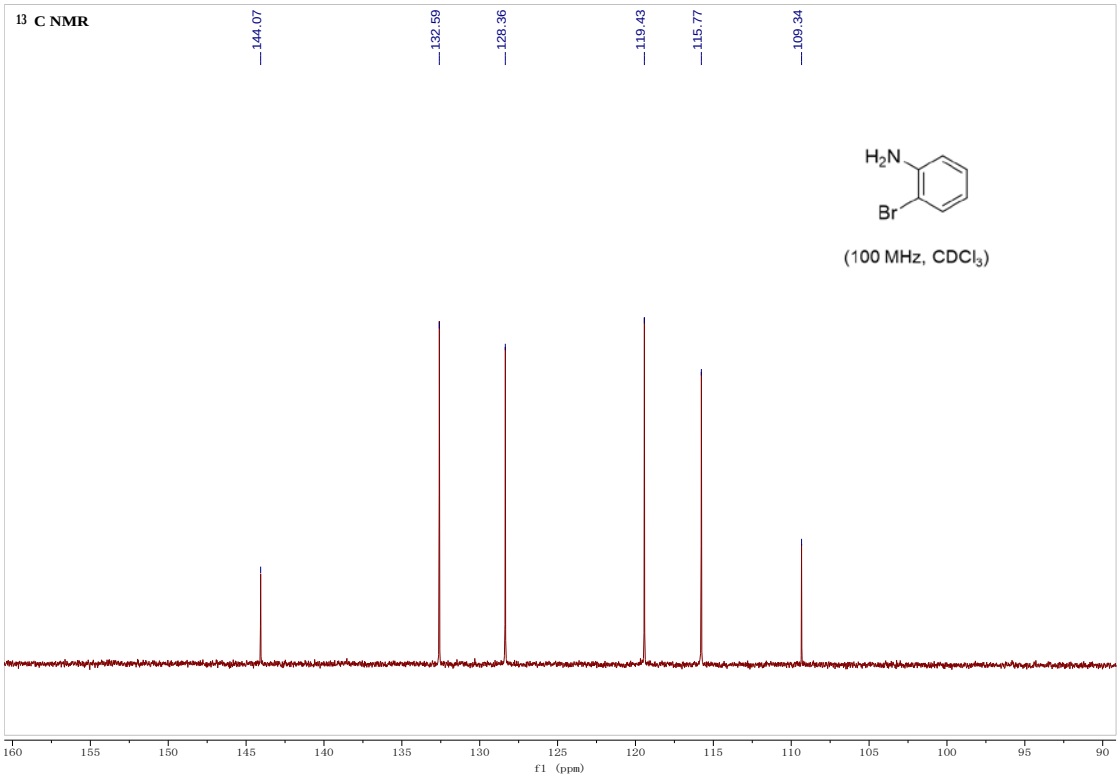


**(5) *p*-Bromoaniline**

$^{1}$H NMR (400 MHz, $CDCl_3$) δ 7.25-7.21 (m, 2H), 6.58-6.54 (m, 2H), 3.66 (s, 2H).

$^{13}$C NMR (100 MHz, $CDCl_3$) δ 145.43, 132.01, 116.72, 110.18.

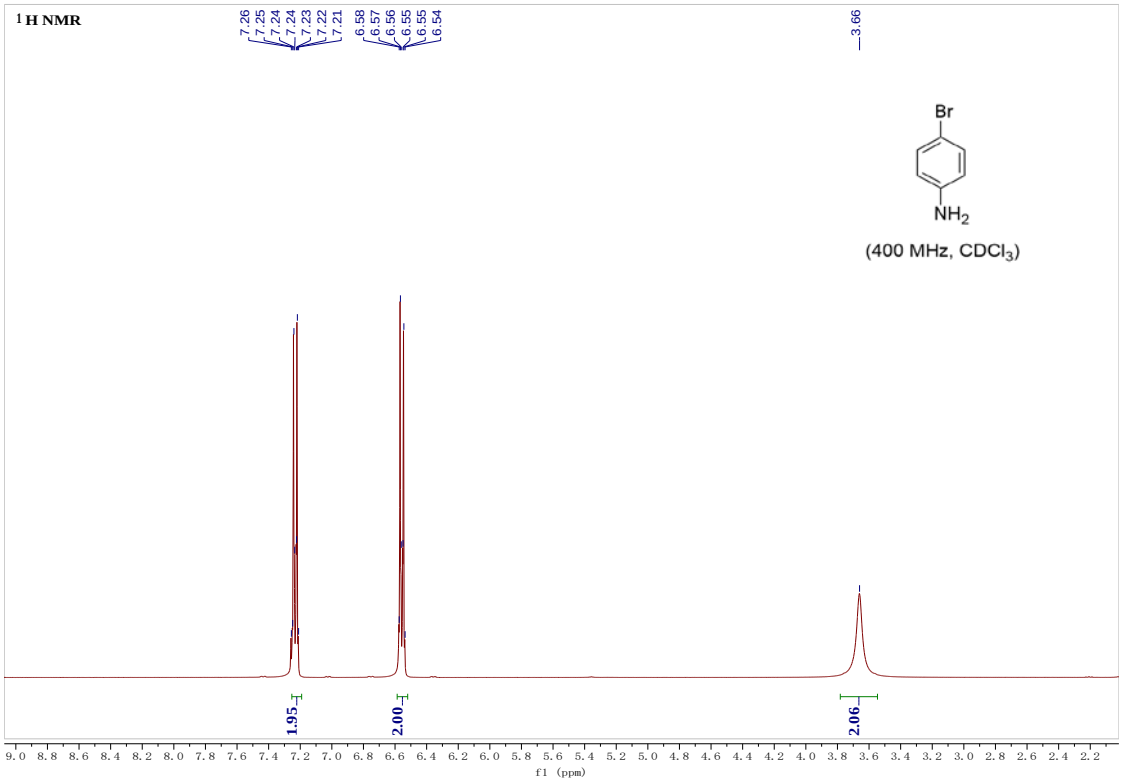

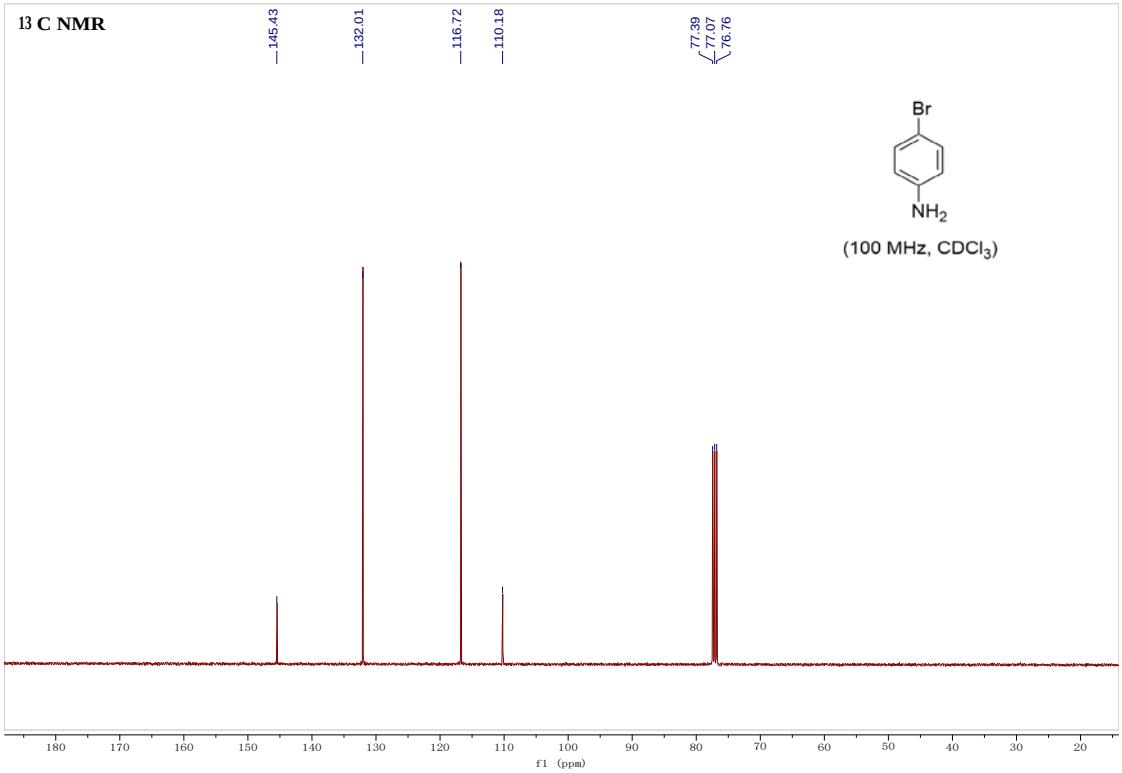


**(6) 2,5-Dibromobenzenamine**

$^{1}$H NMR (400 MHz, $CDCl_3$) δ 7.24 (d, *J* = 8.5 Hz, 1H), 6.90 (d, *J* = 2.2 Hz, 1H), 6.73 (dd, *J* = 8.5, 2.2 Hz, 1H), 4.14 (s, 2H).

$^{13}$C NMR (100 MHz, $CDCl_3$) δ 145.27, 133.62, 122.15, 121.73, 118.10, 107.75.

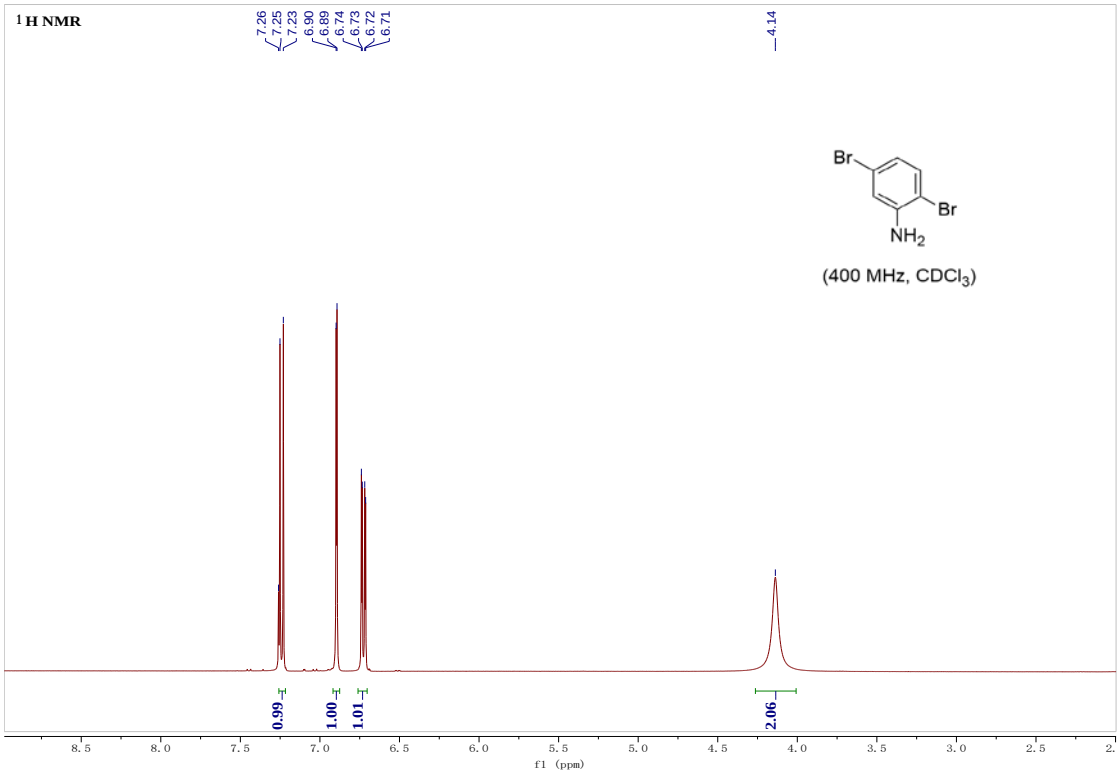

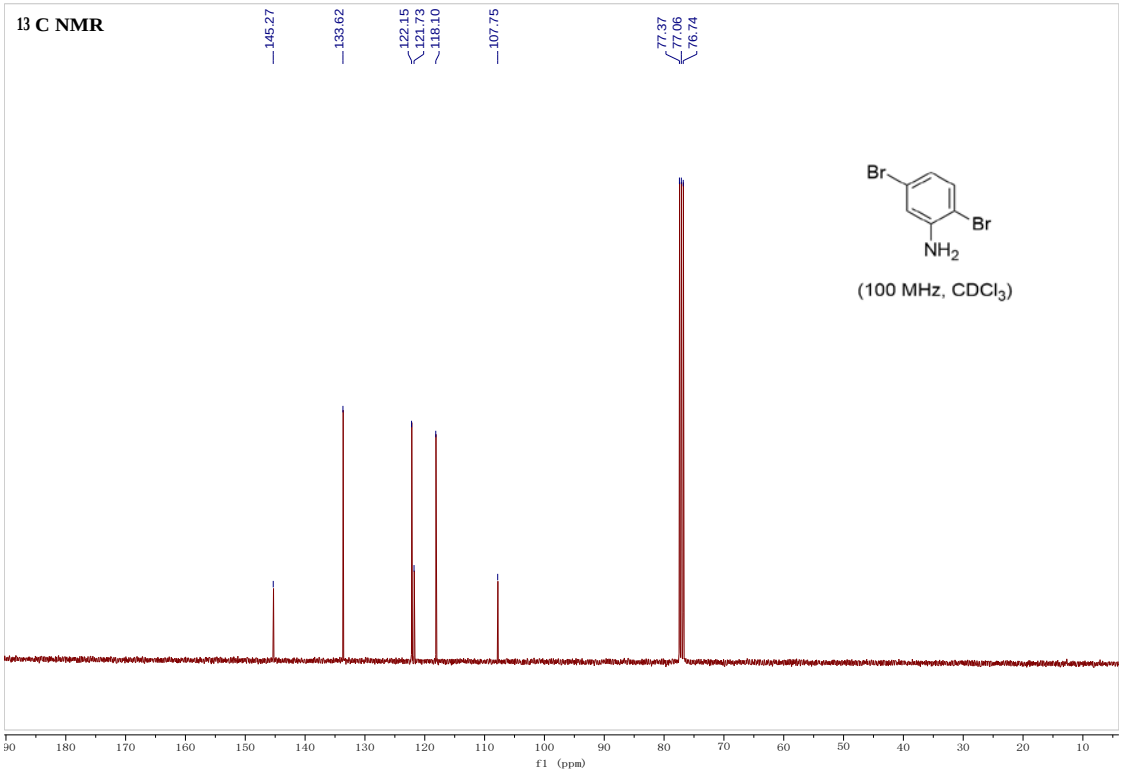


**(7) *p*-Iodoaniline**

$^{1}$H NMR (400 MHz, $CDCl_3$) δ 7.42-7.39 (m, 2H), 6.48-6.45 (m, 2H), 3.59 (s, 2H).

$^{13}$C NMR (100 MHz, $CDCl_3$) δ 146.07, 137.91, 117.31, 79.4.

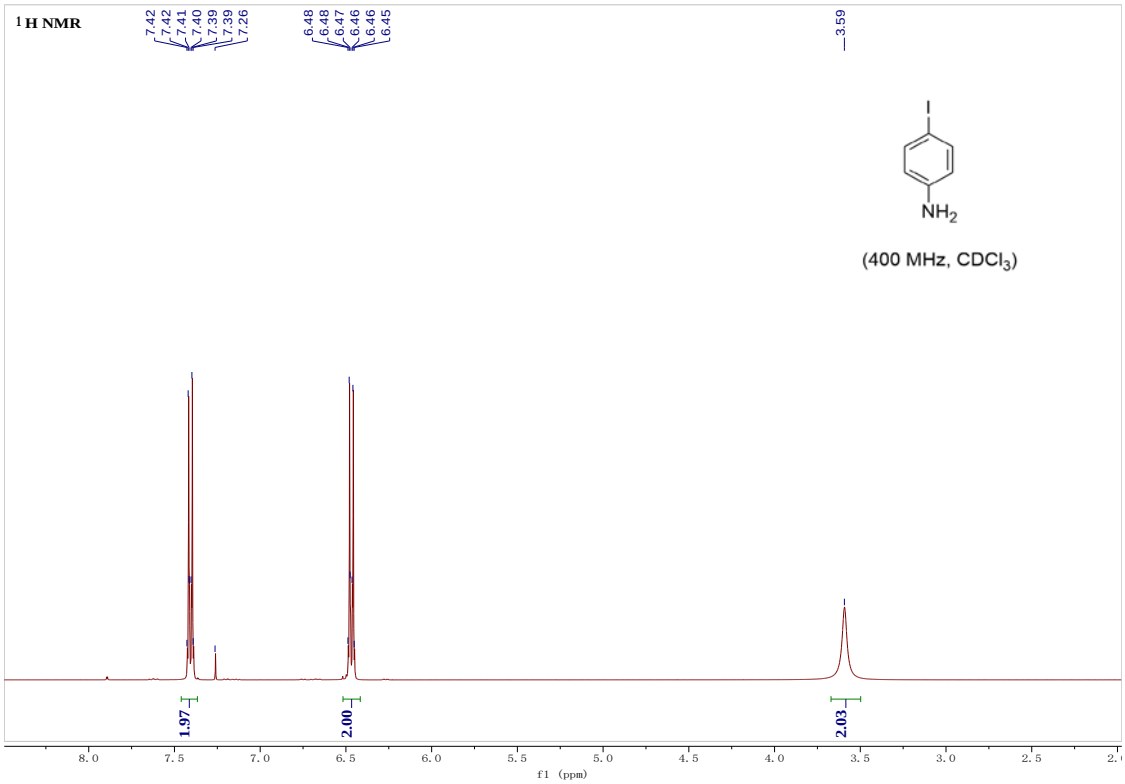

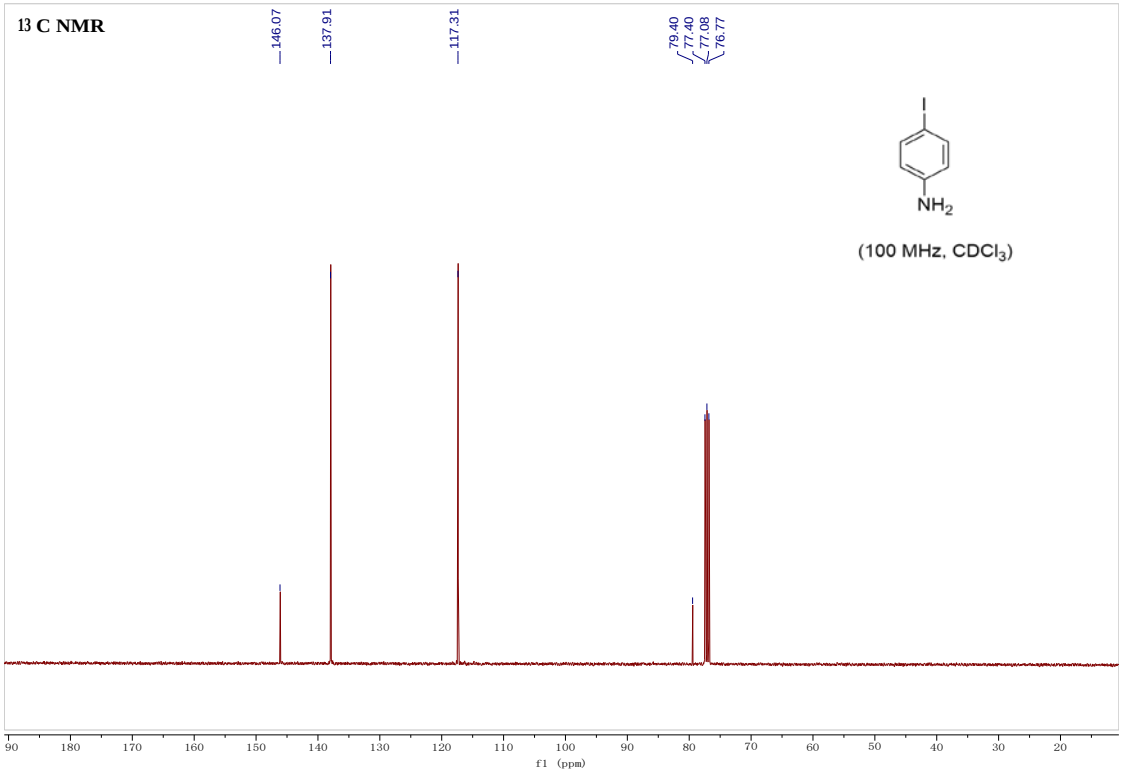


**(8) 4-Aminobenzoic acid**

$^{1}$H NMR (400 MHz, DMSO-$d_6$) δ 11.95 (s, 1H), 7.61 (d, $J$ = 8.7 Hz, 2H), 6.53 (d, $J$ = 8.7 Hz, 2H), 5.87 (s, 2H).

$^{13}$C NMR (100 MHz, DMSO-$d_6$) δ 167.44, 153.09, 131.17, 116.81, 112.50.

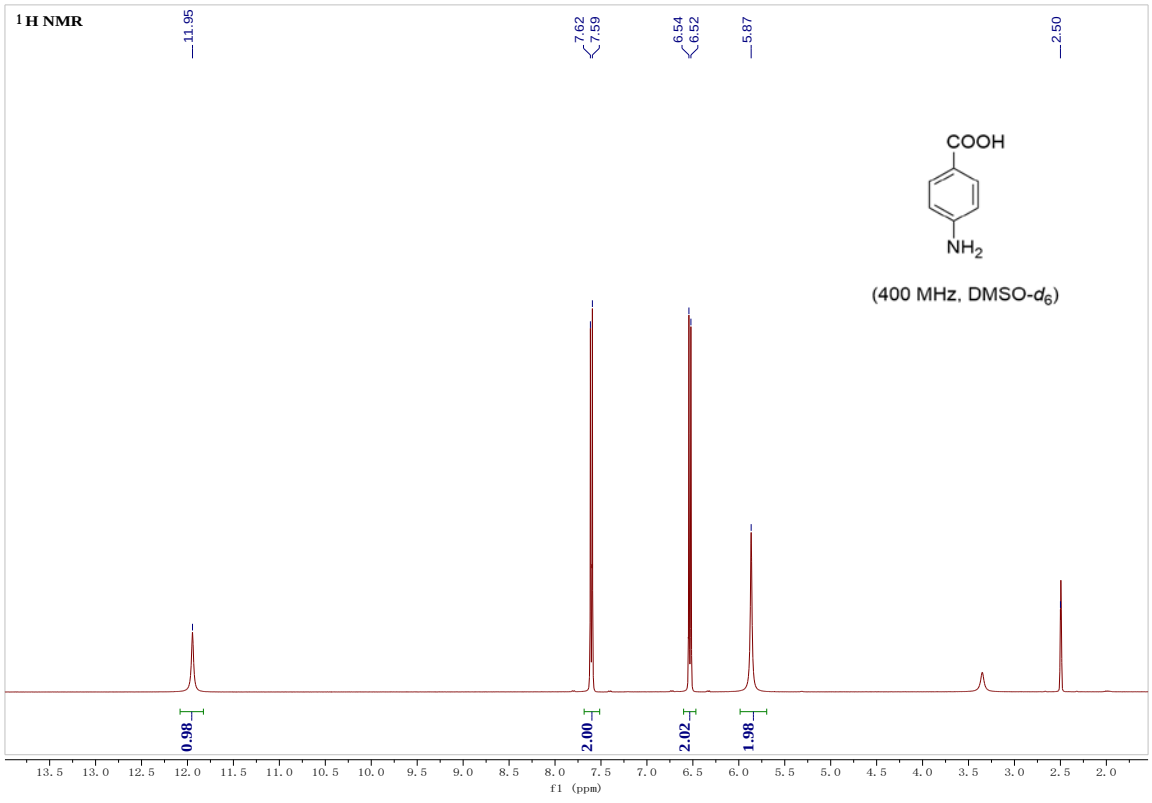

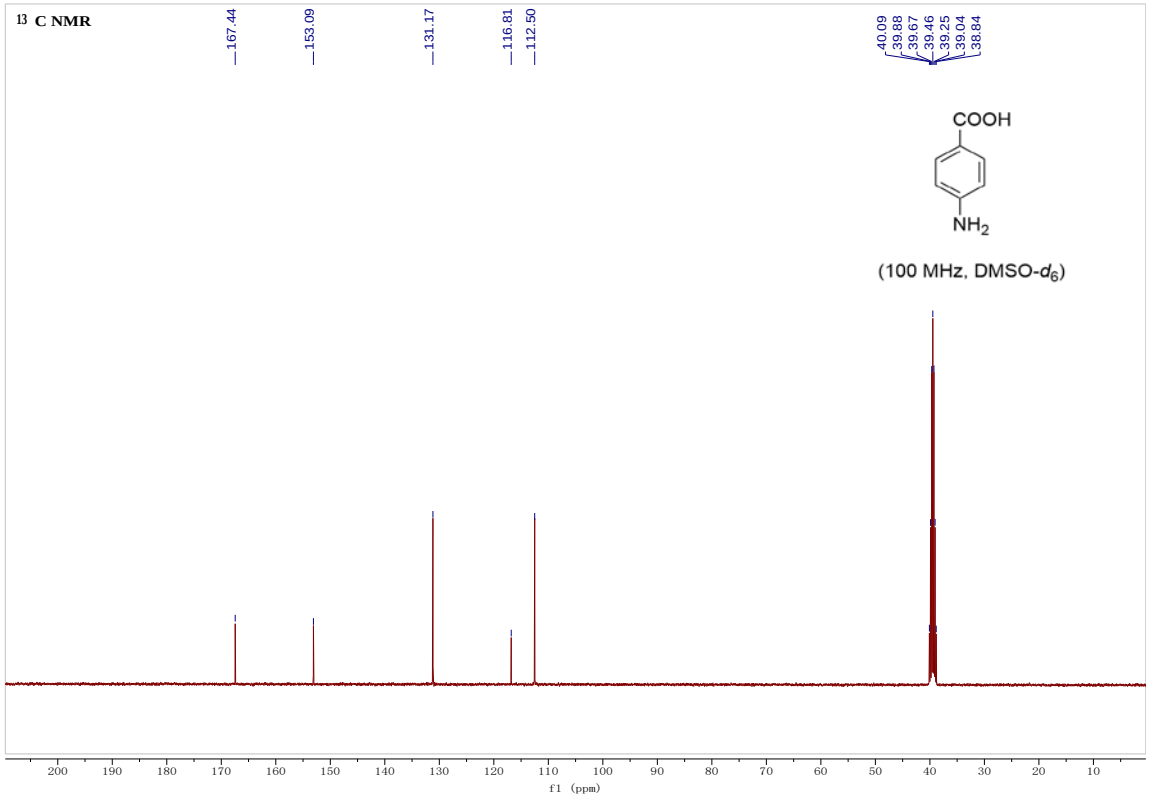


**(9) 4-Aminoacetophenone**

$^{1}$H NMR (400 MHz, $CDCl_3$) δ 7.81 (d, *J* = 8.2 Hz, 2H), 6.65 (d, *J* = 8.3 Hz, 2H), 4.17 (s, 2H), 2.51 (s, 3H).

$^{13}$C NMR (100 MHz, $CDCl_3$) δ 196.53, 151.14, 130.81, 127.84, 115.05, 113.72, 26.11.

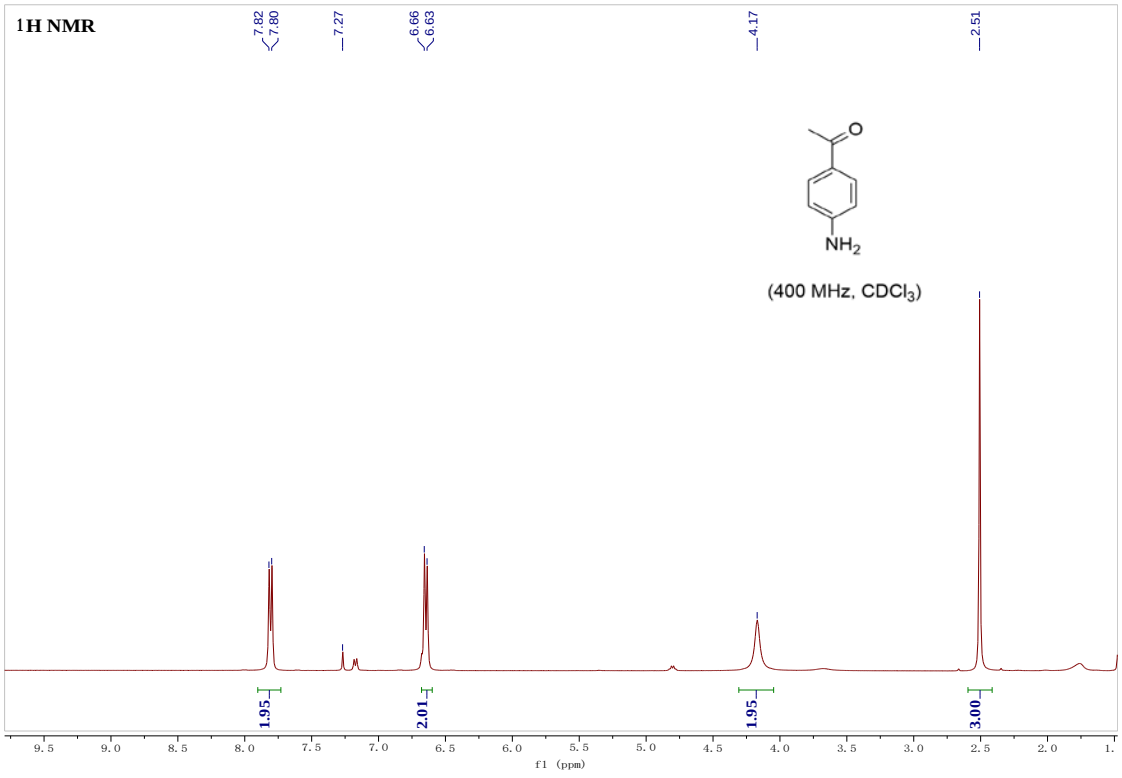

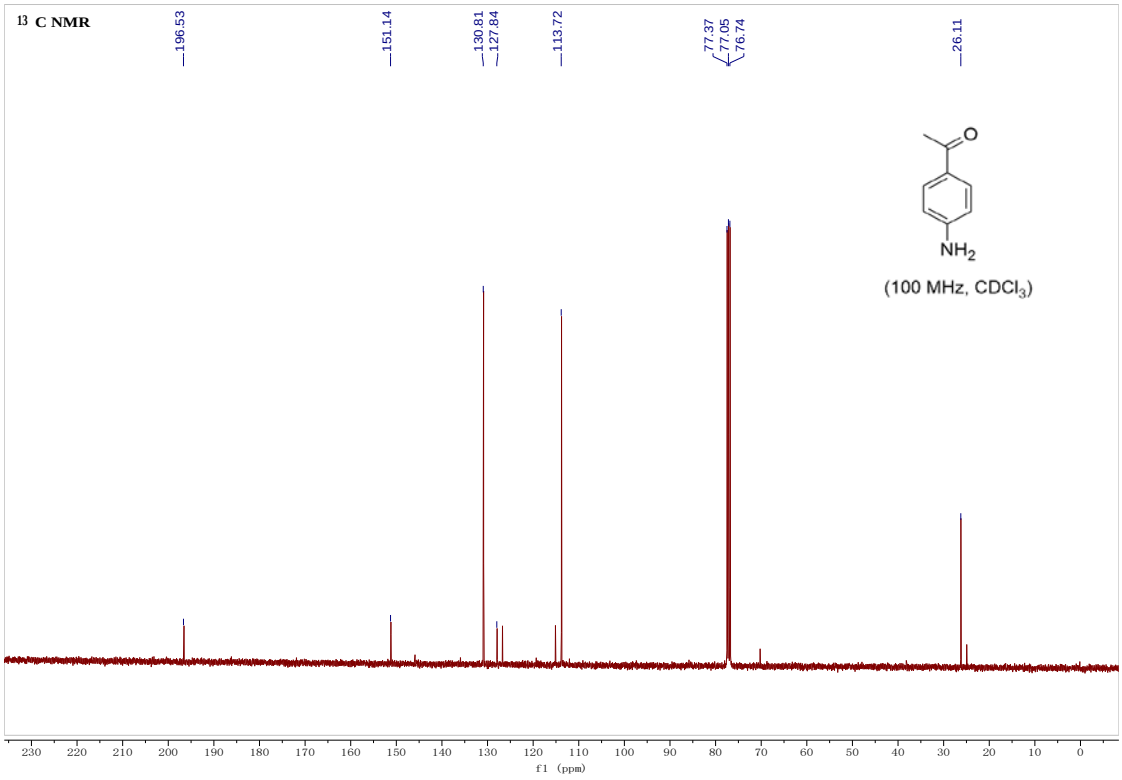


**(10) 4-Aminobenzonitrile**

$^{1}$H NMR (400 MHz, $CDCl_3$) δ 7.42-7.39 (m, 2H), 6.66-6.62 (m, 2H), 4.17 (s, 2H).

$^{13}$C NMR (100 MHz, $CDCl_3$) δ 150.38, 133.82, 120.14, 114.44, 100.22.

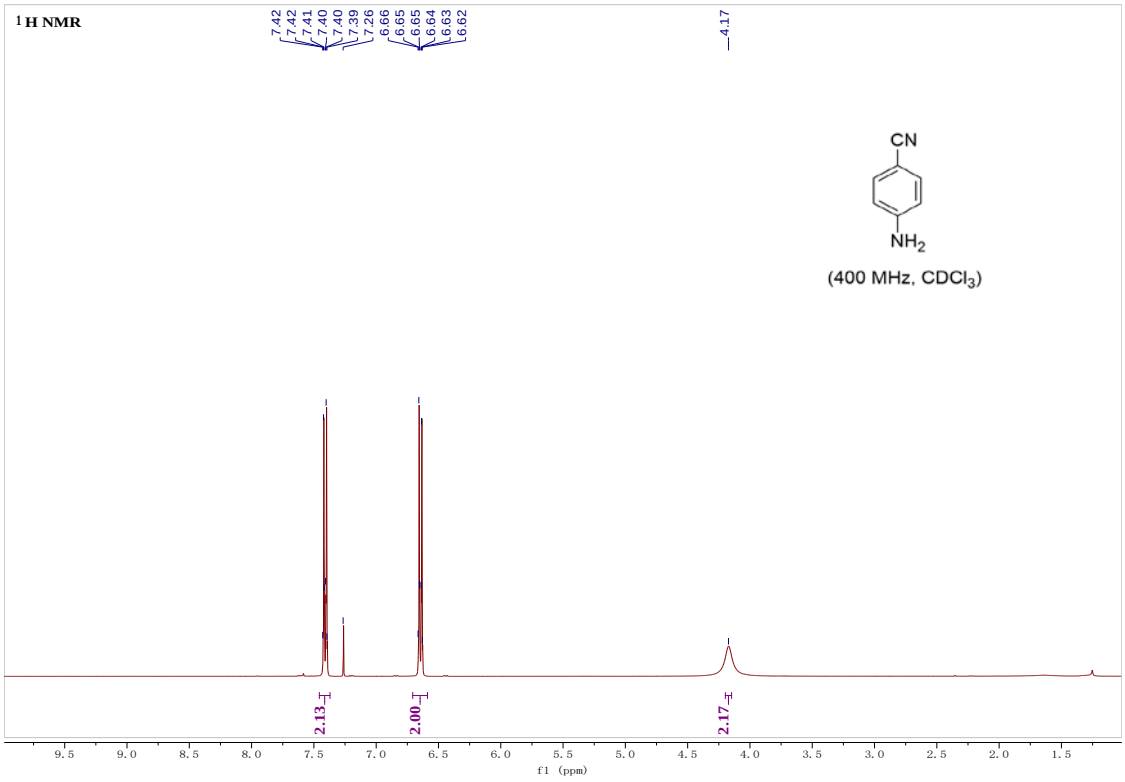

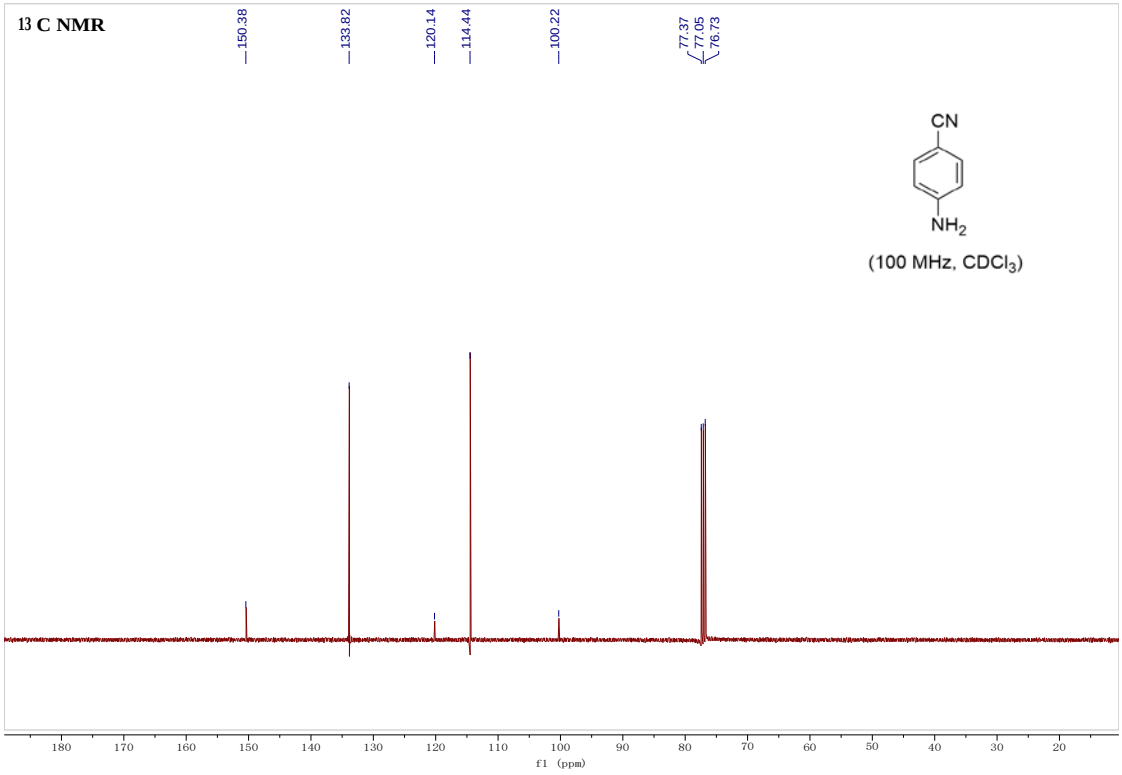


## References


1. Kang Y, Du H, Jiang B, Li H, Guo Y, Amin M A, Sugahara Y, Asahi T, Li H, Yamauchi Y. Microwave one-pot synthesis of CNT-supported amorphous Ni-P alloy nanoparticles with enhanced hydrogenation performance. Journal of Materials Chemistry A, 2022, 10(12): 6560-6568

2. Yang F, Wang M, Liu W, Yang B, Wang Y, Luo J, Tang Y, Hou L, Li Y, Li Z, et al. Atomically dispersed Ni as the active site towards selective hydrogenation of nitroarenes. Green Chemistry, 2019, 21(3): 704-711

3. Li S, Chen X, Wang J, Yao N, Wang J, Cen J, Li X. Construction the Ni@carbon nanostructure with dual-reaction surfaces for the selective hydrogenation reaction. Applied Surface Science, 2019, 489: 786-795

4. She W, Qi T, Cui M, Yan P, Ng S W, Li W, Li G. High catalytic performance of a $CeO_2$-supported Ni catalyst for hydrogenation of nitroarenes, fabricated via coordination-assisted strategy. ACS Applied Materials & Interfaces, 2018, 10(17): 14698-14707

5. Tang B, Song W, Yang E, Zhao X. MOF-derived Ni-based nanocomposites as robust catalysts for chemoselective hydrogenation of functionalized nitro compounds. RSC Advances, 2017, 7(3): 1531-1539

6. Li F, Ma R, Cao B, Liang J, Song H, Song H. Effect of loading method on selective hydrogenation of chloronitrobenzenes over amorphous Ni-B/CNTs catalysts. Catalysis Communications, 2016, 80: 1-4

7. Hahn G, Ewert J-K, Denner C, Tilgner D, Kempe R. A reusable mesoporous nickel nanocomposite catalyst for the selective hydrogenation of nitroarenes in the presence of sensitive functional groups. ChemCatChem, 2016, 8(15): 2461-2465

8. Huang L, Tang F, Hao F, Zhao H, Liu W, Lv Y, Liu P, Xiong W, Luo H. Tuning the electron density of metal nickel via interfacial electron transfer in Ni/MCM-41 for efficient and selective catalytic hydrogenation of halogenated nitroarenes. ACS Sustainable Chemistry & Engineering, 2022, 10(9): 2947-2959

9. Huang L, Lv Y, Liu S, Cui H, Zhao Z, Zhao H, Liu P, Xiong W, Hao F, Luo H. Non-noble metal Ni nanoparticles supported on highly dispersed $TiO_2$-modified activated carbon as an efficient and recyclable catalyst for the hydrogenation of

halogenated aromatic nitro compounds under mild conditions. Industrial & Engineering Chemistry Research, 2020, 59(4): 1422-1435

10. Pan H, Peng Y, Lu X, He J, He L, Wang C, Yue F, Zhang H, Zhou D, Xia Q. Well-constructed Ni@CN material derived from di-ligands Ni-MOF to catalyze mild hydrogenation of nitroarenes. Molecular Catalysis, 2020, 485: 110838